

## Enhanced photocatalytic activity of titania–silica mixed oxide prepared via basic hydrolyzation

Chao Xie<sup>a</sup>, Zili Xu<sup>a,\*</sup>, Qiuqing Yang<sup>a</sup>, Baoyong Xue<sup>a</sup>,  
Yaoguo Du<sup>a</sup>, Jiahua Zhang<sup>b</sup>

<sup>a</sup>College of Environment and Resources, Jilin University, Changchun 130023, China

<sup>b</sup>Laboratory of Excited State Processes, Chinese Academy of Science, Changchun 130023, China

Received 22 September 2003; accepted 17 May 2004

### Abstract

Two different synthesis routes were applied to prepare  $\text{TiO}_2\text{-XSiO}_2$  (X denotes mol% of silica in titania–silica mixed oxides) with different silica concentrations by using ammonia water as hydrolysis catalyst. Through comparing the photocatalytic performance of two sets of mixed oxides, we found that the photocatalytic activity of mixed oxides prepared via the route which can promote homogeneity, was significantly enhanced as compared with that of counterparts prepared via the another route, and the highest photocatalytic activity obtained by adding about 9.1 mol% silica into titania was much higher than that of pure  $\text{TiO}_2$ . The mixed oxides were investigated by means of XRD, thermal analysis, UV–vis, FT-IR and XPS. The characterization results suggest that, in comparison with pure  $\text{TiO}_2$ , the mixed oxides exhibit smaller crystallite size and higher thermal stability which can elevate the temperature of anatase to rutile phase transformation due to the addition of silica. Furthermore, Brønsted acidity, which is associated with the formation of Ti–O–Si hetero linkages where tetrahedrally coordinated silica is chemically mixed with the octahedral titania matrix, may be a very important contribution to the enhanced photocatalytic activity of titania–silica mixed oxides as well.

© 2004 Elsevier B.V. All rights reserved.

**Keywords:** Titania–silica mixed oxide; Basic hydrolyzation; Photocatalytic activity; Brønsted acidity

### 1. Introduction

As a promising class of catalysts, titania–silica mixed oxide has attracted considerable attention due to its widespread environmental applications in environment chemistry and pollution control. When  $\text{TiO}_2$  is mixed with a suitable amount of  $\text{SiO}_2$ , the mixed oxide can not only utilize the good catalytic activity of  $\text{TiO}_2$  but also exhibit improved thermal stability and stronger surface acidity [1–6]. For example, Jung and Park [7] reported that the photocatalytic activity of silica-embedded titania was increased by increasing silica concentration and reached a maximum with a Ti/Si ratio of 70/30 at 700 °C. The increased photocatalytic

activity was due to the simultaneous increase of both surface area and thermal stability by embedding silica into titania. Yu and Yu [8] have also reported that the photocatalytic activity of  $\text{TiO}_2/\text{SiO}_2$  composite thin film reached the maximum when about 5 mol% of  $\text{SiO}_2$  was added. They attributed the enhanced photocatalytic activity to the smaller crystal size and the increased surface hydroxyl content on the surface of the films. Additionally, it has been reported by Liu and co-workers that the surface adsorbed water and hydroxyl groups, whose contents are related to the crystallite form, are crucial for photocatalytic reactions and anatase is more active than rutile in adsorbing water and hydroxyl groups [9]. Therefore, it is reasonable that mixing  $\text{TiO}_2$  with  $\text{SiO}_2$  is an effective method to improve the content of surface adsorbed water and hydroxyl groups, and hence, the photocatalytic activity because the phase transformation from anatase to rutile is inhibited due to the enhanced thermal

\* Corresponding author. Tel.: +86 431 5168429/8503995;  
fax: +86 431 8923907.

E-mail address: xuzl@mail.jlu.edu.cn (Z. Xu).

stability of titania–silica mixed oxide. Furthermore, recently they used the chemical vapor deposition (CVD) method to load TiO<sub>2</sub> onto a bigger particle support (silica gel) for the purpose of improving the recovery rate of TiO<sub>2</sub> photocatalysts in the liquid phase [10]. It was found that the amount of titania coating was strongly dependent on the synthesis parameters, such as carrier gas flow and coating time, and the optimum titania loading rate was around 6 wt.% of the TiO<sub>2</sub> bulk concentration. In particular, it has been pointed out that the positive charge imbalance due to tetrahedrally coordinated silica chemically mixing with the non-tetrahedral titania at the molecular level is balanced by a hydroxyl groups, thus producing new Brønsted acidity which is also a very important contribution for the enhanced photocatalytic activity of titania–silica mixed oxide [3,4,11].

Recently, some studies regarding pure TiO<sub>2</sub> have reported that using ammonia water as hydrolysis catalyst can not only suppress the phase transformation but also enhance the surface area [12,13]. However, the effects of basic hydrolysis catalyst on the photocatalytic activity of titania–silica mixed oxide have been less investigated. Furthermore, the photocatalytic activity of titania–silica mixed oxide is intimately related to the hydrolysis route, silica concentration and calcination temperature [1–3,14]. Therefore in this paper, we prepared two sets of mixed oxides with variable silica concentrations by using ammonia water as hydrolysis catalyst via two different synthesis routes, one set prepared through adding Ti sol into Si sol and the second set by simultaneously mixing the Ti sol and Si sol to promote the homogeneity of the mixed oxides. Our aim is to find out the optimum silica concentration with respect to the photocatalytic performance when using basic hydrolysis catalyst and explain the dependence of photocatalytic activity upon composition mainly in terms of the physicochemical properties of titania–silica mixed oxide and the generation of Brønsted acidity which is related to the Ti–O–Si hetero linkages.

## 2. Experimental

### 2.1. Preparation

Two sets of titania–silica mixed oxides were prepared by using ammonia water as the hydrolysis catalyst. Titanium tetrabutoxide and tetraethyl orthosilicate were selected as the source of titania and silica, respectively. Here, we give a typical procedure for the preparation of TiO<sub>2</sub>–9.1% SiO<sub>2</sub>. Firstly, 17.0 ml TBOT was mixed with 5.1 ml acetylacetone and 10.0 ml anhydrous ethanol. Secondly, 1.125 ml TEOS was mixed with the solution containing 10.8 ml bidistilled water, 23.9 ml ammonia water and 20.0 ml anhydrous ethanol under stirring. After a few minutes, this solution changed to opaque white due to the formation of dense Si sol. The final step was to mix the sols of Ti and Si via two different synthesis routes.

*Route A:* Ti sol was added dropwise into the Si sol under stirring

*Route B:* Ti sol and Si sol were simultaneously and slowly added into the beaker containing 10.0 ml anhydrous ethanol under stirring.

When the drops were finished, the beaker was covered by plastic film and aged for 72 h in order to further hydrolyze TBOT and TEOS. Titania–silica mixed oxides with different silica concentrations were obtained by only varying the dosage of TEOS. A pure titania sample was prepared by the route B, except no TEOS was added into the Si sol. Finally, the samples obtained were evaporated and dried under infrared lamp, followed by calcination in the range of 400–800 °C for 2 h, and then, ground into fine powders.

### 2.2. Characterization

The crystalline phases of the samples prepared were characterized by a Bruker D8 GADDS X-ray diffractometer using Cu K $\alpha$  radiation ( $\lambda = 1.54056 \text{ \AA}$ ). In addition, The crystalline sizes  $D$  were estimated from the width of lines in the X-ray pattern with the aid of the Scherrer formula:  $D = K\lambda/(\beta\cos\theta)$ , where  $\lambda$  is the wavelength of the X-ray used,  $\beta$  is the width of the line at the half-maximum intensity, and  $K$  is a constant. Thermogravimetric analysis (TG/DTA) was carried out using a NETZSCH STA 449C instrument. FT-IR spectra for the samples were obtained by utilizing a Nicolet Impact 410 Fourier transform infrared spectrophotometer. UV–vis spectra were recorded on a Perkin–Elmer Lambda 20 spectrometer. X-ray photoelectron spectroscopy (XPS) measurements were performed in a VG ESCALAB MKII X-ray photoelectron spectrometer. The X-ray source emitted Mg K $\alpha$  radiation (1253.6 eV). For all of the binding energy of Ti and O obtained, the pressure was maintained at  $6.3 \times 10^{-7}$  Pa. Binding energies were calibrated with respect to the signal for adventitious carbon (binding energy = 284.6 eV).

### 2.3. Photocatalytic activity tests

The photocatalytic activity experiments on the catalysts for the oxidation of heptane were carried out at room temperature using a 300 ml cylindrical quartz tube. In the experiment, 0.1 g of sample was spread uniformly over the internal surface of the reactor. After this, the reactor was vacuum-packed and suitable amounts of heptane (0.1%), oxygen (20%) were injected into the reactor. Then, ultra-purity nitrogen was mixed with the reactants in the reactor to one atmospheric pressure. Prior to the illumination, which was provided by a 400 W high-pressure mercury lamp producing a strong peak centered at 365 nm, the catalysts were allowed to reach adsorption balance with the reactant gas. Subsequently, the content of heptane in the reactor was measured with a Hewlett–Packard 4890 gas chromatograph equipped with a flame ionization detector (FID).

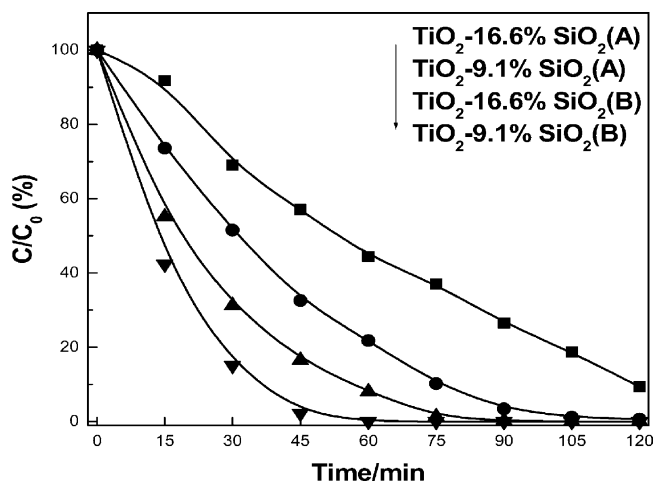


Fig. 1. The comparison of photocatalytic activity of titania-silica mixed oxides prepared via two different synthesis routes calcined at 600 °C (A and B in the parenthesis represent route A and route B, respectively).

### 3. Results and discussion

#### 3.1. Choice of the synthesis route

The photocatalytic activities of  $\text{TiO}_2$ -16.6%  $\text{SiO}_2$  and  $\text{TiO}_2$ -9.1%  $\text{SiO}_2$  prepared via two different synthesis routes are shown in Fig. 1. It is clear that the photocatalytic activity of the mixed oxides prepared by route B was much higher than that of counterparts prepared via route A. As we have known, photocatalytic activity of mixed oxides is strongly related to textural properties which are dependent on the goodness of molecular-scale mixing, or in other words homogeneity [1–3]. When the sols of Ti and Si are mixed, rapid hydrolysis and condensation of Ti-alkoxide lead to the formation of Ti-rich cores and the subsequent development of Si-rich shell. As for route A, since Ti sol was added into Si sol, at the initial phase of reaction very dense Si-rich shell was formed and obscured much of the surface active sites in that the Si/Ti ratio was rather high in the reaction solution. With the further addition of Ti-alkoxide, the Si/Ti ratio was dropped down, meaning that silica cannot be mixed with Ti-rich cores uniformly. However, in the case of route B, Si sol and Ti sol were simultaneously and slowly added, which can keep the Si/Ti ratio in the reaction solution essentially constant during the whole period of reaction, and thereafter, guarantee to form more homogeneous titania-silica mixed oxides relative to those prepared via route A. So, it is

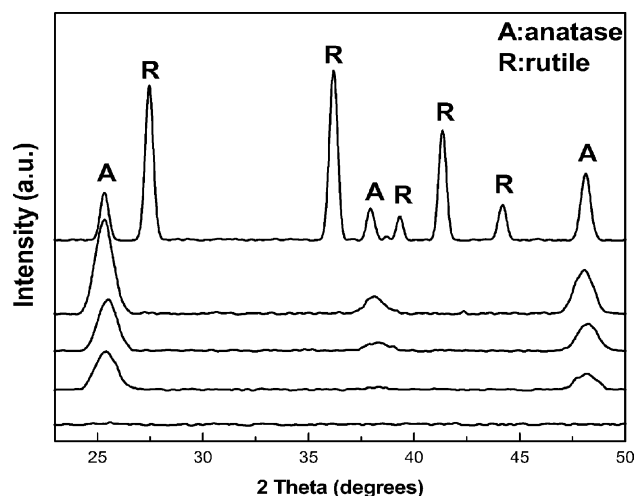


Fig. 2. XRD patterns of titania-silica mixed oxides and pure  $\text{TiO}_2$  calcined at 600 °C. From the top to the bottom: pure  $\text{TiO}_2$ ,  $\text{TiO}_2$ -4.7%  $\text{SiO}_2$ ,  $\text{TiO}_2$ -9.1%  $\text{SiO}_2$ ,  $\text{TiO}_2$ -16.6%  $\text{SiO}_2$  and  $\text{TiO}_2$ -50%  $\text{SiO}_2$ .

reasonable that the mixed oxides prepared via route B had higher photocatalytic activity than those via route A. Based on the photocatalytic performance, our later work will be focused on the mixed oxides prepared via route B.

#### 3.2. XRD analysis

XRD patterns of titania-silica mixed oxides and pure  $\text{TiO}_2$  as a function of calcination temperature were obtained. Here, we take the patterns of catalysts calcined at 600 °C as a model and show them in Fig. 2. The crystalline sizes and crystal phases are listed in Table 1. It can be seen from Table 1 that after calcination at 400 °C for 2 h  $\text{TiO}_2$ -16.6%  $\text{SiO}_2$ ,  $\text{TiO}_2$ -9.1%  $\text{SiO}_2$ ,  $\text{TiO}_2$ -4.7%  $\text{SiO}_2$  and pure  $\text{TiO}_2$  has been transformed into anatase phase, while  $\text{TiO}_2$ -50%  $\text{SiO}_2$  were still amorphous. As the calcination temperature was further increased to 600 °C, pure  $\text{TiO}_2$  has been converted into the mixture of anatase and rutile (major phase). But, we noted that  $\text{TiO}_2$ -50%  $\text{SiO}_2$  was transformed into anatase at 800 °C. It can also be observed that the crystalline size of mixed oxide was significantly decreased as a small amount of silica was added with respect to pure  $\text{TiO}_2$  calcined at same temperature. Moreover, the crystalline size was further decreased with more silica added. Therefore, it can be concluded that the addition of silica can inhibit the growth of crystalline size and suppress the phase transformation from anatase to rutile.

Table 1

Crystallite sizes (nm) and crystal phases of titania-silica mixed oxides as a function of calcination temperature<sup>a</sup>

Calcination temperature (°C)	$\text{TiO}_2$ -50% $\text{SiO}_2$	$\text{TiO}_2$ -16.6% $\text{SiO}_2$	$\text{TiO}_2$ -9.1% $\text{SiO}_2$	$\text{TiO}_2$ -4.7% $\text{SiO}_2$	Pure $\text{TiO}_2$
400	– (Am)	12.8 (A)	13.5 (A)	17.3 (A)	26.5 (A)
600	– (Am)	15.9 (A)	17.6 (A)	24.7 (A)	39.5 (A+R)
800	14.5 (A)	16.2 (A)	20.3 (A+R)	28.1 (A + R)	55.3 (R)

<sup>a</sup> Am, A and R in the parenthesis represent amorphous, anatase, and rutile, respectively.

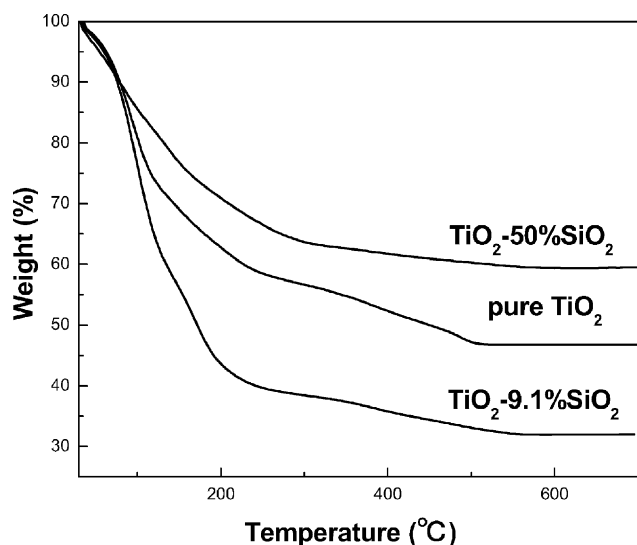


Fig. 3. TGA curves of  $\text{TiO}_2$ -50%  $\text{SiO}_2$ ,  $\text{TiO}_2$ -9.1%  $\text{SiO}_2$  and pure  $\text{TiO}_2$  precursors.

### 3.3. Thermal analysis

Fig. 3 shows the TGA curves of  $\text{TiO}_2$ -50%  $\text{SiO}_2$ ,  $\text{TiO}_2$ -9.1%  $\text{SiO}_2$  and pure  $\text{TiO}_2$ . It can be seen that an obvious weight loss at around 100 °C, corresponding to the endothermic peak at about 100 °C in Fig. 4, was due to the desorption of physically bonded water and surface dehydroxylation [15]. With increasing the temperature, the TGA curves became smooth and the weight was completely constant at around 600 °C, illustrating that the organic residues in the mixed oxides were completely removed above 600 °C. Fig. 4 shows the DTA curves of  $\text{TiO}_2$ -50%  $\text{SiO}_2$ ,  $\text{TiO}_2$ -9.1%  $\text{SiO}_2$  and pure  $\text{TiO}_2$ , respectively. For all samples there was a broad exothermic peak between 340 and 400 °C. From the XRD results listed in Table 1, we can see that  $\text{TiO}_2$ -50%  $\text{SiO}_2$  was not converted to anatase up to 600 °C, but

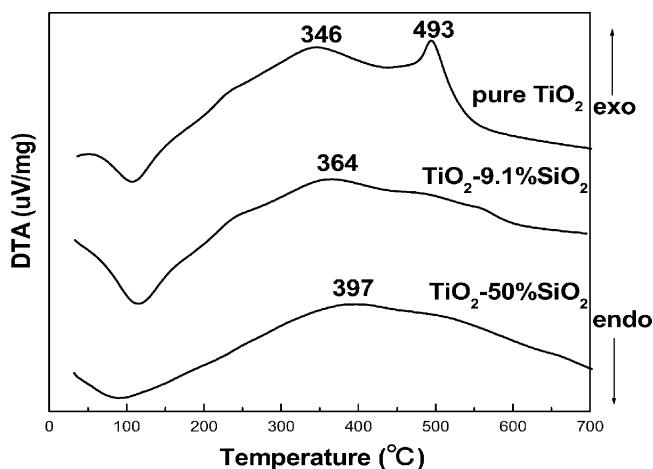


Fig. 4. DTA curves of  $\text{TiO}_2$ -50%  $\text{SiO}_2$ ,  $\text{TiO}_2$ -9.1%  $\text{SiO}_2$  and pure  $\text{TiO}_2$  precursors.

$\text{TiO}_2$ -9.1%  $\text{SiO}_2$  and pure  $\text{TiO}_2$  have been transformed into anatase phase below 400 °C. So, the broad exothermic peak at round 397 °C could be attributed to the combustion of organic residues in the case of  $\text{TiO}_2$ -50%  $\text{SiO}_2$ . However, the peaks at around 364 and 346 °C for  $\text{TiO}_2$ -9.1%  $\text{SiO}_2$  and pure  $\text{TiO}_2$  could not be simply explained like this. These two exothermic peaks should belong to the elimination of organic residues and crystallization [16]. It is interesting to note that the exothermic peak at 493 °C for pure  $\text{TiO}_2$ , associated with the phase transformation from anatase to rutile, was not observed in the curves of the  $\text{TiO}_2$ -50%  $\text{SiO}_2$  and  $\text{TiO}_2$ -9.1%  $\text{SiO}_2$  below 700 °C. This illustrates that the phase transformation is suppressed due to the addition of silica, which agrees with the results of XRD very well.

### 3.4. FT-IR spectroscopy

FT-IR spectra of  $\text{TiO}_2$ -50%  $\text{SiO}_2$  calcined at 400, 600 and 800 °C are depicted in Fig. 5. The bands at 466 and 1087  $\text{cm}^{-1}$  are assigned to the Si-O-Si bending modes and asymmetric  $V_{\text{as}}(\text{Si-O-Si})$  stretching vibration, respectively [15,17]. However, the band at 810  $\text{cm}^{-1}$  which is attributed to symmetric  $V_{\text{s}}(\text{Si-O-Si})$  observed in the IR spectra of pure  $\text{SiO}_2$  depicted in Fig. 6, does not appear in the spectra of titania-silica mixed oxides. The band at 948  $\text{cm}^{-1}$  can be associated with the Ti-O-Si linkages [1,18], which evidences the interaction between titania and silica at molecular-scale that can evidently enhance the surface properties and photocatalytic activity [4]. The peaks at 1623 and 3434  $\text{cm}^{-1}$  assigned to the stretching vibration of OH group and molecular  $\text{H}_2\text{O}$  were obviously removed as the calcination temperature raised up. Especially, those two bands were hardly observed at 800 °C. This demonstrates that the surface of mixed oxide became clean and the density of surface bulk defects was reduced with increasing the calcination temperature [7]. Furthermore,

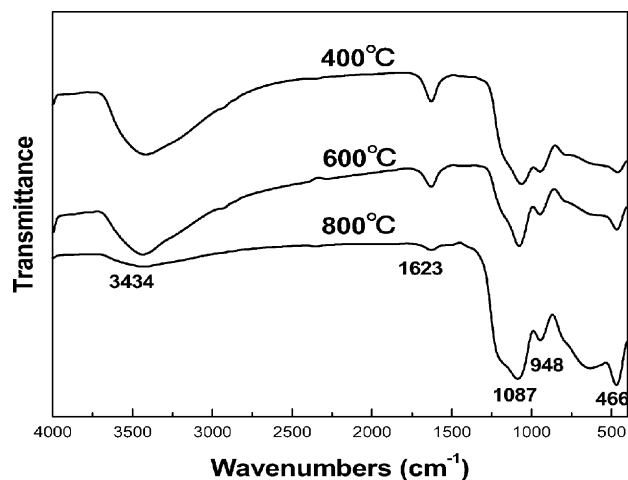


Fig. 5. FT-IR spectra of  $\text{TiO}_2$ -50%  $\text{SiO}_2$  as a function of calcination temperature.

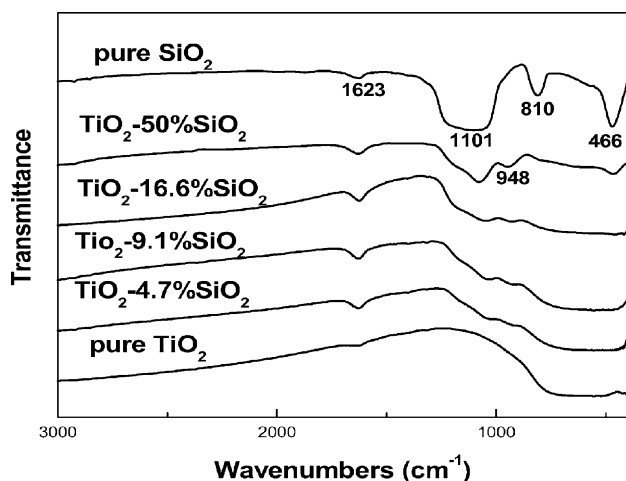


Fig. 6. FT-IR spectra of pure  $\text{SiO}_2$ , pure  $\text{TiO}_2$  and titania-silica mixed oxides calcined at  $600^\circ\text{C}$ .

higher temperature will be helpful not only for completely decomposing the organic residues covered on the surface active sites, but also for improving the homogeneity of mixed oxides because parts of surface hydroxyl groups will combine to lose a water molecular and form Ti–O–Si hetero linkages which are associated with the generation of Brønsted acidity [6,19]. On the other hand, higher calcination temperature also means that the surface on which the water molecules were adsorbed and the surface hydroxyl groups helpful for improving photocatalytic activity were reduced [7]. Therefore, the mixed oxides must be calcined at a suitable temperature in order to obtain good photocatalytic activity. Fig. 6 exhibits the spectra for the titania-silica mixed oxides with variable silica concentrations calcined at  $600^\circ\text{C}$ . It can be seen that for all the mixed oxides the band assigned to Ti–O–Si hetero linkage can be observed, while this band of  $\text{TiO}_2$ -9.1%  $\text{SiO}_2$  and  $\text{TiO}_2$ -4.7%  $\text{SiO}_2$  obviously shifted to the low wavenumber and became broader. This fact evidences the structure change of Ti–O–Si hetero linkages that can result in the enhanced surface acidity, which is coincided with the results reported by Sohn and Jang [20]. The intensity of the broad absorption band between  $500$  and  $1000\text{ cm}^{-1}$  attributed to Ti–O–Ti linkages in segregated  $\text{TiO}_2$  nanoparticles, was decreased with the addition of silica and disappeared in the case of  $\text{TiO}_2$ -50%  $\text{SiO}_2$ , implying that Ti atoms gradually changed from an octahedral environment to a tetrahedral environment because more Ti atoms were incorporated into tetrahedral sites in the silica network [21].

### 3.5. UV-vis spectroscopy

Fig. 7 depicts the UV-vis spectra of titania-silica mixed oxides calcined at  $600^\circ\text{C}$ . The absorption band near  $240\text{ nm}$  (labeled as A), which can be observed in the case of  $\text{TiO}_2$ -9.1%  $\text{SiO}_2$  and  $\text{TiO}_2$ -4.7%  $\text{SiO}_2$ , illustrates that titania possessed an octahedral coordination in the mixed oxides

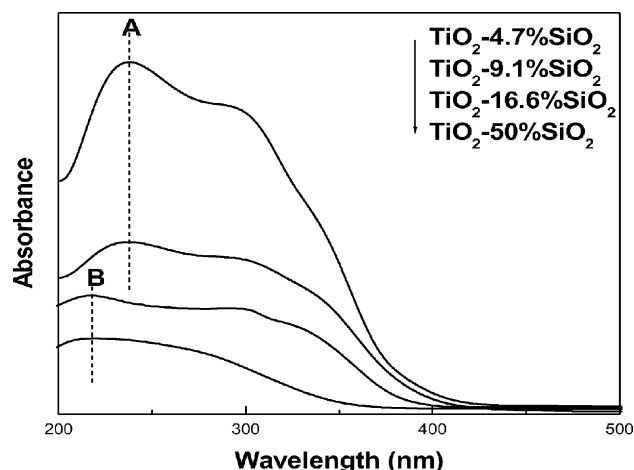


Fig. 7. UV-vis spectra of titania-silica mixed oxides calcined at  $600^\circ\text{C}$ .

with lower silica concentration ( $\text{Si} \leq 9.1\text{ mol}\%$ ). It is noteworthy that this band near  $240\text{ nm}$  disappeared and a new absorption band between  $210$  and  $220\text{ nm}$  (labeled as B) appeared in the spectra of  $\text{TiO}_2$ -16.6%  $\text{SiO}_2$  and  $\text{TiO}_2$ -50%  $\text{SiO}_2$ , illustrating that titania gradually changed from an octahedral environment to a tetrahedral environment with increasing silica concentration [22–25]. This hypothesis is in accordance with the result of FT-IR which revealed that the coordination change of titania with the increase of silica concentration. Furthermore, we can infer that for the mixed oxides ( $\text{Si} \leq 9.1\text{ mol}\%$ ) possessing Ti–O–Si linkages, where titania retained its octahedral coordination and was mixed with the tetrahedrally coordinated silica, Brønsted acidity was formed and its strength should be increased as the concentration of silica was increased because more silica can react with titania to form Ti–O–Si linkages and reached the maximum at around  $\text{TiO}_2$ -9.1%  $\text{SiO}_2$ . This is in agreement with the previous study, which suggested that the highest Brønsted acidity was achieved when about  $10\text{ mol}\%$  silica was added into titania [11]. With the further increase of silica concentration, the strength of Brønsted acidity may be reduced in that titania gradually changed from an octahedral environment to a tetrahedral environment. Moreover, Fig. 7 clearly shows that the band edge, especially for  $\text{TiO}_2$ -50%  $\text{SiO}_2$ , was significantly blue-shifted due to the well-known quantum size effect [25–27]. Therefore, we can conclude that the crystalline size of mixed oxides was significantly decreased with the addition of silica, in good agreement with the results listed in Table 1. Meanwhile, the blue-shift is also a confirmation that the titania gradually change from octahedral coordination to tetrahedral coordination with increasing silica concentration [24,25].

### 3.6. X-ray photoelectron spectroscopy

Fig. 8 exhibits the O 1s spectra of  $\text{TiO}_2$ -50%  $\text{SiO}_2$  calcined at  $600^\circ\text{C}$ . Curve-fitting result suggested that there



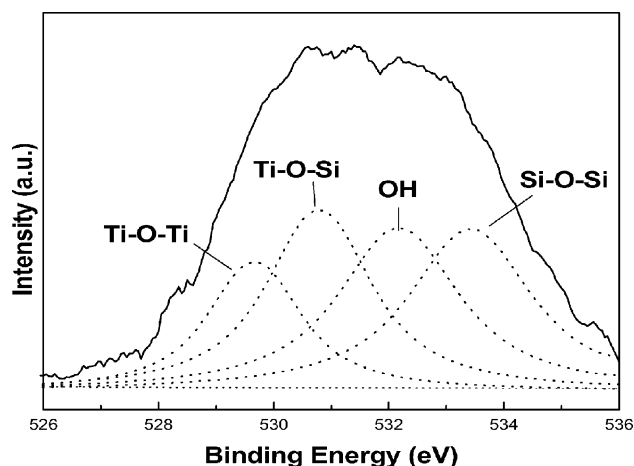


Fig. 8. XPS of O 1s for  $\text{TiO}_2$ -50%  $\text{SiO}_2$  calcined at 600 °C.

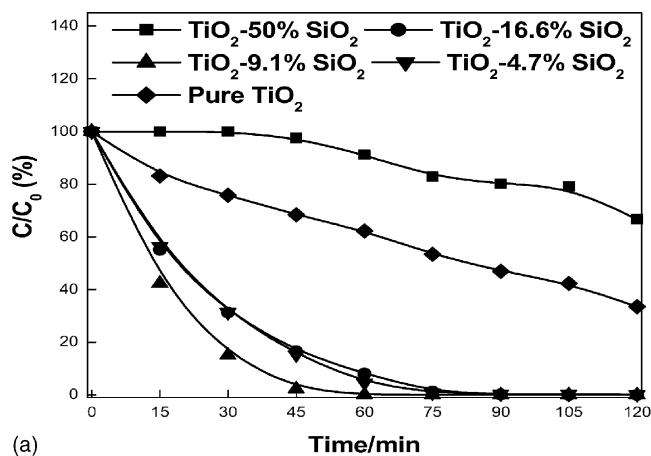
should exist four kinds of oxygen in the mixed oxide. The peaks at around 529.6, 531.0 and 533.3 eV can be attributed to the oxygen in Ti–O–Ti, Ti–O–Si and Si–O–Si linkages [18,19], respectively, while the peak at around 532.0 eV can be assigned to surface hydroxyl [28]. From Table 2, we found that at same calcination temperature the surface hydroxyl content of  $\text{TiO}_2$ -50%  $\text{SiO}_2$  is higher than that of  $\text{TiO}_2$ -9.1%  $\text{SiO}_2$ , implying that the addition of silica is beneficial for obtaining higher content of surface hydroxyl. Meanwhile, the surface hydroxyl content decreased as the calcination temperature increased for the  $\text{TiO}_2$ -9.1%  $\text{SiO}_2$ .

The values of Ti  $2p_{3/2}$  of both  $\text{TiO}_2$ -50%  $\text{SiO}_2$  calcined at 600 °C and  $\text{TiO}_2$ -9.1%  $\text{SiO}_2$  calcined at 400, 600 and 800 °C are listed in Table 2. According to the previous studies, the Ti 2p  $2/3$  binding energy of pure  $\text{TiO}_2$  is 458.5 eV [1,18]. The upward shift of Ti 2p  $2/3$  value of titania–silica mixed oxide can also confirm the formation of the Ti–O–Si hetero linkages [18]. This is because the formation of Ti–O–Si linkages can significantly change the electronic structure of Ti species in titania–silica mixed oxide, and increase the effective positive charge on the Ti species due to the decrease of the electron density around Ti species resulting from the greater electronegativity of Si via O acting on Ti [1,29]. At the same time, it is interesting to note that the increase in the Ti 2p  $2/3$  value of  $\text{TiO}_2$ -9.1%  $\text{SiO}_2$  as a function of calcination temperature, implying that higher temperature can promote the generation of Ti–O–Si hetero linkages.

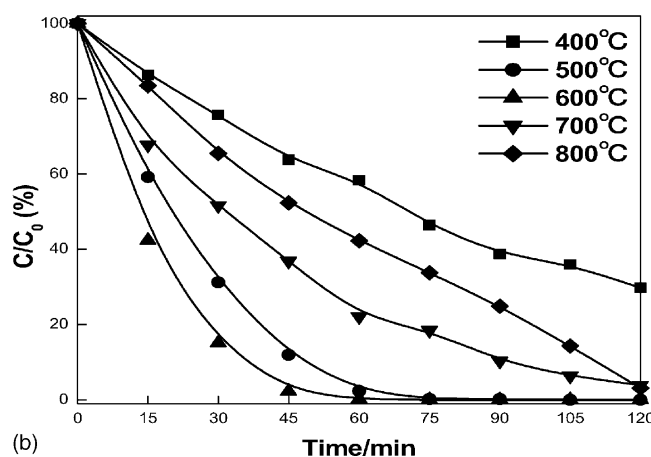
Table 2

The surface hydroxyl contents and the values of Ti  $2p_{3/2}$  of titania–silica mixed oxides

Catalysts	Calcination temperature (°C)	Hydroxyl content	Ti $2p_{3/2}$ (eV)
$\text{TiO}_2$ -50% $\text{SiO}_2$	600	24.78%	459.3
$\text{TiO}_2$ -9.1% $\text{SiO}_2$	400	26.48%	458.8
$\text{TiO}_2$ -9.1% $\text{SiO}_2$	600	21.70%	458.9
$\text{TiO}_2$ -9.1% $\text{SiO}_2$	800	17.44%	459.2



(a)



(b)

Fig. 9. The comparison of photocatalytic activity with irradiation time. (a) Titania–silica mixed oxides and pure  $\text{TiO}_2$  calcined at 600 °C; (b)  $\text{TiO}_2$ -9.1%  $\text{SiO}_2$  calcined at different temperatures.

### 3.7. Photocatalytic activity tests

Fig. 9a demonstrates how the photocatalytic activities of titania–silica mixed oxide varied with silica concentration. It can be seen that the photocatalytic activity of mixed oxides ( $\text{Si} \leq 16.6$  mol%) was much higher than that of pure  $\text{TiO}_2$  and the maximum activity occurred at  $\text{TiO}_2$ -9.1%  $\text{SiO}_2$ . The enhanced photocatalytic activity of titania–silica mixed oxide can be ascribed to the following three reasons. Firstly, anatase phase of titania was formed at higher temperature (600 °C) when silica was added into titania. It has been reported that the photocatalytic activity of anatase phase is

superior to rutile phase [9,30,31]. Meanwhile, higher temperature can completely decompose the organic residues on the catalyst surface, promote the degree of crystallinity and effectively remove the bulk defects which can lower the photocatalytic activity in that they provide sites for the recombination of the photogenerated electron–hole pairs [32]. Secondly, crystalline size of mixed oxide was decreased with respect to pure  $\text{TiO}_2$  calcined at same temperature. In general, the smaller crystalline size means that the chances of recombination for photogenerated electron–hole pairs decrease because of their faster arrival at the reaction site on the catalyst surface [33], and band gap is increased which can cause an increase in the oxidizing potential of the photogenerated holes [1]. Finally, Brønsted acidity is generated when a suitable amount of silica is added. In order to effectively demonstrate how the Brønsted acidity can improve the photocatalytic activity of titania–silica mixed oxide, it is necessary for us to understand the basic mechanism of photocatalytic reaction which takes place at the surface of catalyst. When photocatalyst is illuminated by the light stronger than its band gap energy, electron–hole pairs diffuse out to the surface of the photocatalyst. Electrons and holes can recombine or participate in the chemical reaction with electron donors and acceptors. In the absence of suitable electron and hole scavengers, the recombination of electron–hole pairs will occur within a few nanoseconds [30]. However, suitable addition of silica can produce stronger Brønsted acidity, which is helpful for improving the content of surface hydroxyl groups [6]. As we have known, surface hydroxyl groups can accept photo-induced holes to form OH radicals and then oxidize absorbed molecules. Hence, the enhanced activities of  $\text{TiO}_2$ –9.1%  $\text{SiO}_2$  and  $\text{TiO}_2$ –4.7%  $\text{SiO}_2$  can be mainly attributed to the Brønsted acidity, which is agreement with the report by Liu et al. that the enhanced photocatalytic activity over Ti-rich mixed oxides was attributed to the generation of Brønsted acidity [4]. Furthermore, we consider that the stronger Brønsted acidity of  $\text{TiO}_2$ –9.1%  $\text{SiO}_2$  was responsible for its higher photocatalytic activity in contrast to  $\text{TiO}_2$ –4.7%  $\text{SiO}_2$ . Since, titania gradually changed from an octahedral environment to a tetrahedral environment with increasing silica concentration, so the enhanced photocatalytic activity of  $\text{TiO}_2$ –16.6%  $\text{SiO}_2$  was mainly due to the formation of anatase phase of  $\text{TiO}_2$  with smaller crystalline size, instead of Brønsted acidity. We can assume that as silica concentration was increased to 50%, no or a very small amount of Brønsted acidity was generated since almost all titania were changed to tetrahedral coordination. In addition, the surface photoactive sites were occupied by too much silica, which can significantly decrease the utilizing efficiency of input energy for titania because silica is a kind of insular and has no photocatalytic activity. On the other hand, from Table 1 we can see that at 600 °C, it was still in amorphous, illustrating that the mixed oxide has poor crystallinity. Therefore, it is reasonable that the  $\text{TiO}_2$ –50%  $\text{SiO}_2$  has the lowest photocatalytic activity.

Fig. 9b shows the photocatalytic activity of  $\text{TiO}_2$ –9.1%  $\text{SiO}_2$  as a function of calcination temperature. Some researchers found that the photoactivity of  $\text{TiO}_2$  is proportional to the content of hydroxyl groups on the surface [34,35]. The result of XPS, which suggested that the content of surface hydroxyl groups of  $\text{TiO}_2$ –9.1%  $\text{SiO}_2$  calcined at 400 °C was higher as compared with that calcined at 600 °C, seems to hint that  $\text{TiO}_2$ –9.1%  $\text{SiO}_2$  calcined at 400 °C should have higher photocatalytic activity. However, contrary to our expectation the mixed oxide calcined at 600 °C had the highest photocatalytic activity. From the result of TGA in Fig. 4, we can see that  $\text{TiO}_2$ –9.1%  $\text{SiO}_2$  had a slight weight loss between 300 and 500 °C, indicating that there were some organic residues in  $\text{TiO}_2$ –9.1%  $\text{SiO}_2$  which can lower the photocatalytic activity below 500 °C. As the temperature was increased up to 600 °C, the organic residues were completely removed since there was no weight loss. So the photocatalytic activity was significantly enhanced. The highest photocatalytic activity was also due to its higher degree of crystallinity and reduced bulk defects compared to the mixed oxides calcined below 600 °C [32]. As the calcination temperature was above 600 °C, the content of surface hydroxyl groups will be obviously reduced and the crystalline size will be increased. Therefore, the photocatalytic activity of  $\text{TiO}_2$ –9.1%  $\text{SiO}_2$  calcined at 700 and 800 °C was retarded.

#### 4. Conclusions

The photocatalytic activity of two sets of titania–silica mixed oxides, which were prepared by using ammonia water as hydrolysis catalyst via two different synthesis routes, was studied through photodegradation of heptane. The obvious difference between the photocatalytic performances in the two sets of mixed oxides confirms that the photocatalytic activity is intimately related to the goodness of molecular-scale mixing, or in other words homogeneity. Titania–silica mixed oxides ( $\text{Si} \leq 16.6 \text{ mol}\%$ ) have much higher photocatalytic activity than pure  $\text{TiO}_2$ . This is because suitable addition of silica into titania can efficiently enhance the thermal stability which increases the temperature of phase transformation and allow us to calcine titania–silica mixed oxides at higher temperature to obtain anatase phase of titania with high degree of crystallinity and smaller crystalline size, and reduce the bulk defects. Moreover, Brønsted acidity, which is concluded from the results of FT-IR and UV–vis, should be a very important contribution to the highest photocatalytic activity of  $\text{TiO}_2$ –9.1%  $\text{SiO}_2$ . However, when 50 mol% silica was added into mixed oxides, the activity of catalyst will be evidently dropped down because the transformation from amorphous to anatase is inhibited and the surface active sites are covered by too much inactive silica.

## Acknowledgment

This work was supported by a grant from the National Natural Science Foundation of china (No. 20277015).

## References

- [1] X. Gao, I.E. Wachs, *Catal. Today* 51 (1999) 233.
- [2] J.B. Miller, E.I. Ko, *Catal. Today* 35 (1997) 269.
- [3] J.B. Johnston, S.T. Miller, E.I. Ko, *J. Catal.* 150 (1994) 311.
- [4] Z. Liu, J. Tabora, R.J. Davis, *J. Catal.* 149 (1994) 117.
- [5] C. Anderson, A.J. Bard, *J. Phys. Chem.* 99 (1995) 9882.
- [6] X. Fu, L.A. Clark, Q. Yang, M.A. Anderson, *Environ. Sci. Technol.* 30 (1996) 647.
- [7] K.Y. Jung, S.B. Park, *Appl. Catal. B* 25 (2000) 249.
- [8] J. Yu, J.C. Yu, *J. Sol-Gel Sci. Tech.* 24 (2002) 95.
- [9] Z. Ding, Q. Liu, P.F. Greenfield, *J. Phys. Chem. B* 104 (2000) 4815.
- [10] Z. Ding, X. Hu, Q. Lu, Po-Lock Yue, P.F. Greenfield, *Langmuir* 16 (2000) 6216.
- [11] P.K. Doolin, S. Alerasool, D.J. Zalewski, J.F. Hoffman, *Catal. Lett.* 25 (1994) 209.
- [12] J. Yu, J.C. Yu, M.K.-P. Leung, W. Ho, B. Cheng, X. Zhao, J. Zhao, *J. Catal.* 217 (2003) 69.
- [13] K.M.S. Khalil, M.I. Zaki, *Powder Technol.* 92 (1997) 233.
- [14] R. Hutter, T. Mallat, A. Baiker, *J. Catal.* 153 (1995) 177.
- [15] D.C.M. Dutoit, M. Schneider, A. Baiker, *J. Catal.* 153 (1995) 165.
- [16] K.M.S. Khalil, M.I. Zaki, *Powder Technol.* 120 (2001) 256.
- [17] K.M.S. Khalil, A.A. Elsamahy, M.S. Elanany, *J. Colloid Interface Sci.* 249 (2002) 359.
- [18] X. Gao, S.R. Bare, J.L.G. Fierro, M.A. Banares, I.E. Wachs, *J. Phys. Chem. B.* 102 (1998) 5653.
- [19] R. Castillo, B. Koch, P. Ruiz, B. Delmon, *J. Catal.* 161 (1996) 524.
- [20] J.R. Sohn, H.J. Jang, *J. Catal.* 132 (1991) 563.
- [21] J.B. Miller, E.I. Ko, *J. Catal.* 159 (1996) 58.
- [22] A. Tuel, L.G. Hubert-Pfalzgaf, *J. Catal.* 217 (2003) 343.
- [23] A. Zecchina, G. Spoto, S. Bordiga, A. Ferrero, G. Petrini, G. Leofanti, M. Padovan, *Stud. Surf. Sci. Catal.* 69 (1991) 251.
- [24] C. Beck, T. Mallat, T. Burgi, A. Baiker, *J. Catal.* 204 (2001) 428.
- [25] M. Galan-Fereres, L.T. Alemany, R. Mariscal, M.A. Banares, J.A. Anderson, J.L.G. Fierro, *Chem. Mater.* 7 (1995) 1342.
- [26] G. Lassaletta, A. Fernandez, J.P. Espinos, A.R. Gonzalez, *J. Phys. Chem.* 99 (1995) 1484.
- [27] Z. Ding, H. Zhu, P.F. Greenfield, *J. Colloid Interface Sci.* 238 (2001) 267.
- [28] Z. Xu, J. Shang, C. Liu, C. Kang, H. Guo, Y. Du, *Mater. Sci. Eng. B* 56 (1999) 211.
- [29] Y. Lin, T. Wang, Y. Jin, *Powder Technol.* 123 (2002) 194.
- [30] M.R. Hoffmann, S.T. Martin, W. Choi, D.W. Bahnemann, *Chem. Rev.* 95 (1995) 69.
- [31] A. Fujishima, T.N. Rao, D.A. Tryk, *J. Photochem. Photobiol. C* 1 (2000) 1.
- [32] K.Y. Jung, S.B. Park, *J. Photochem. Photobiol. A* 127 (1999) 117.
- [33] R.I. Bickley, F.S. Stone, *J. Catal.* 31 (1973) 389.
- [34] A.H. Boonsta, C.A.H.A. Mutsaers, *J. Phys. Chem.* 79 (1975) 1694.
- [35] E. Pelizzetti, C. Minero, *Electrochim. Acta* 38 (1993) 47.